Geosciences

AIMS Geosciences, 5(2): 235–264.
DOI: 10.3934/geosci.2019.2.235
Received: 12 February 2019
Accepted: 15 May 2019
Published: 27 May 2019

http://www.aimspress.com/journal/geosciences

*Research article*

# Characterization and engineering properties of AMU Morasko soft clay

**Robert Radaszewski and Jędrzej Wierzbicki***

Institute of Geology, Adam Mickiewicz University, Poznan, Poland

* **Correspondence:** Eamil: jwi@amu.edu.pl; Tel: +48604912848.

**Abstract:** AMU Morasko soft clay is the normally consolidated, postglacial clayey silty sand to sandy clay, deposited during the last glaciation (Weichselian) within the marginal zone of end moraine of Posnanian Phase. These soils are characterized by low plasticity, high porosity and are fully saturated, therefore, from a geotechnical point of view they can be defined as soft clays. The over 10 meter thick complex of clayey glacial sediments is covered with fine and medium sands with single grains of gravel of the so-called first sandur level from the youngest glaciation. This kind of sediments are very common in the area of north-western Poland and, due to high compressibility, become a problematic subsoil for the shallow foundations. The high porosity and saturation also causes significant problems in obtaining high quality samples for laboratory tests. This means that in situ tests are very often the only possible and economically justifiable test methods. Extended investigations carried out on these clays, which provide reliable correlations between in situ and laboratory test results, will be very useful.

For the purpose of this research paper, a wide variety of *in situ* (CPTU, DMT, FVT) and laboratory (physical properties, direct shear, oedometer) tests have been carried out on the material found at the depth of up to 16 m, in the area of 8 ha, within the campus of Adam Mickiewicz University (AMU) in Poznań, Poland. Preliminary investigations (performed four years ago) showed high uniformity of the test site. The current laboratory tests were carried out on both high quality natural samples and reconstructed samples. The rate effect on the results of some of the tests was also investigated. The obtained results allowed to present a wide geological and engineering characterization of these interesting glacial deposits.

**Keywords:** soft clay; test site; compressibility; strength; *in situ* test

## 1. Introduction

The AMU Morasko test site, the origin of the presented test results, is located in the north-western part of Poland at the northern border of Poznan (Figure 1) on the campus of Adam Mickiewicz University. Its contractually defined geographical coordinates 16°54′55″ ÷ 16°55′06″ E and 52°27′56″ ÷ 52°28′17″ N defined an area of c. 8 ha in total. It is located in the close vicinity of the Morasko Meteorite Nature Reserve which owes its name to iron meteors that fell c. 5–6 k years ago [1].

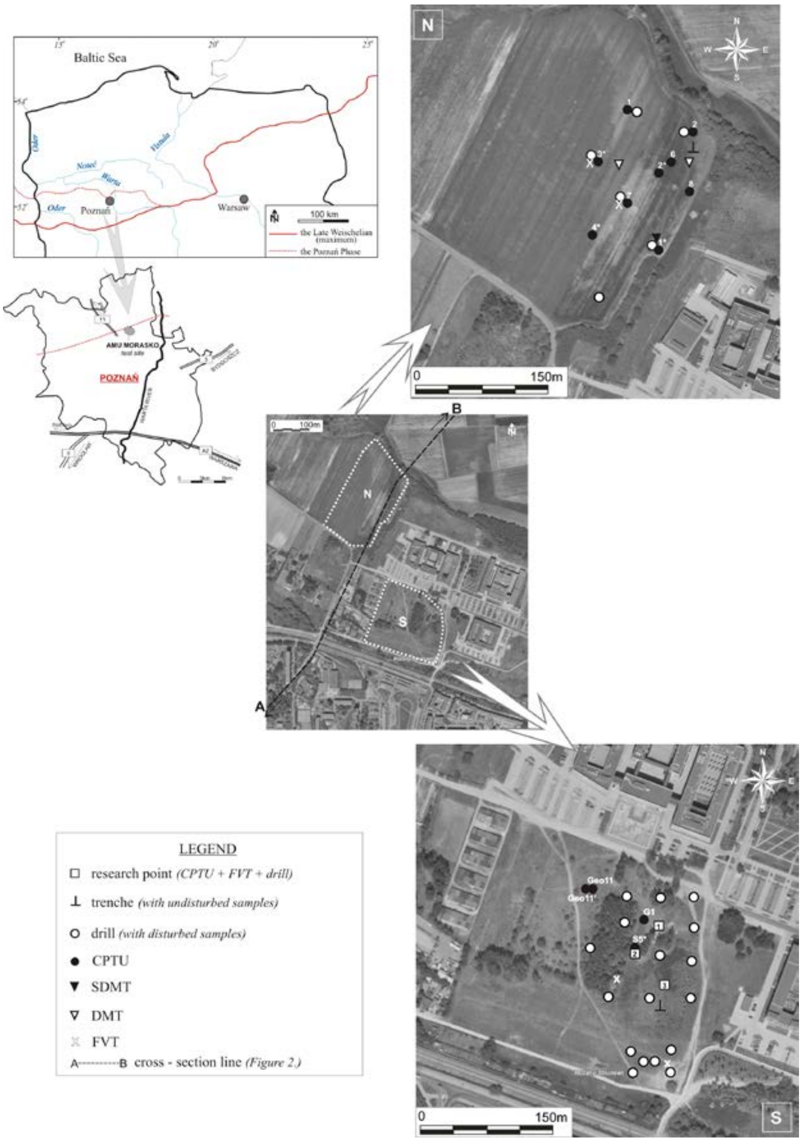


**Figure 1.** Location of the AMU Morasko test site and tests carried out in the area having taken into account the scope of the Poznanian Phase of the Weichselian glaciation.

This region is characterized by young glacial terrain common for the late Pleistocene [2,3], mostly related to the so-called Poznanian Phase of the Weichselian glaciation which reaches the edge of a terminal moraine in the direct vicinity of the described area (Figure 2). Geotechnically analyzed soils should be classified as normally consolidated (NC). The potential preconsolidation effect [4], should be linked to the natural location variability of underground waters found on the analyzed area from the moment of their formation until (during the decline of the Pleistocene) the modern times, also with possible cementation zones. Nevertheless, these soils were not mechanically overloaded in their geological history.

The first geological studies conducted within the current test site borders of its southern part (Figure 1) took place in May of 2014 while implementing geotechnical documentation required to build the foundations of a 5-storey student dormitory which was being designed at the time (Table 1).

**Table 1.** The scope of the performed tests on the AMU Morasko test site.

| Year | Investigations |
|---|---|
| 2014 | • Cone penetration tests (CPTU) |
| | • Drillings and remoulded sample collection |
| | • Laboratory tests (physical properties) |
| 2015 | • Formal start of AMU Morasko test site |
| 2016 | • Micropiles |
| | • Cone penetration tests (CPTU) |
| | • Flat dilatometer test (DMT) |
| | • Drillings and remoulded sample collection |
| | • CPTU dissipation test at northern part of test site |
| 2017 | • Cone penetration tests (CPTU)—different manufacturers |
| | • Cone penetration tests (CPTU) with test rate of 0.5 cm/s |
| | • Downhole seismic test (SDMT) |
| | • Flat dilatometer test (DMT) |
| | • CPTU dissipation test at southern part of test site |
| | • Field vane test FVT & SLVT[1] |
| | • Direct shear apparatus (different test rates) |
| | • Oedometric tests (IL & CRS) |
| | • Laboratory tests (physical properties) |
| 2018 | • Drillings and remoulded sample collection |
| | • Block samples from trenches |
| | • Field vane test FVT (different test rates) |
| | • Direct shear apparatus (different test rates) |
| | • Oedometric tests (IL & CRS) |
| | • Atterberg limits (3 methods) |

Rotary drillings and cone penetration tests performed at the depth of up to 10 m in the subsoil documented the presence of a 6–8 meter wide thick layer (its bottom layer was not reached), which consisted of specific mineral soils of low plasticity and low geotechnical parameters. The high homogeneity of these soils with lateral and horizontal spreading turned out to be surprising and

[1] The SLVT is a probe, which is a modification of a light dynamic probe (DPL). They differ in terms of changing the cone tip to a cross tip (the same as in FVT) and equipping the probe with a dynamometric key for to measure the rotation moment. This method is not normalized, however, it is often used by Polish geotechnical companies. The most significant differences of SLVT as compared to the standard FVT probe are as follows: (1) no casing pipes around the rods connecting the probe head to the cross ending (2) greater rate of shearing, although its measurement is not very precise.

interesting at the same time. This fact became a direct cause of creating a test site in this region of a relatively large area of ~3 ha, with the span of 150 to 200 m in 2015. It was built with the consent of the owner, i.e. Adam Mickiewicz University authorities.

Test micropiles were installed at the site in 2016 and their aim was to assess the efficiency of a method which reinforces the subsoil for the construction works that were to come. Since losing the chance to examine such geologically interesting area was imminent, because of its planned construction works, in order to assess the geological structure of the neighboring plots tests were conducted. North became the logical direction of the research process because of the development of the neighboring land. The conducted reconnaissance cone penetration tests proved that the layer of low plasticity soils of limited bearing capacity and similar thickness goes on towards the north over the distance of 400 m from the border of the current test site. Thus, in 2016 the test site was expanded c. 4.5 ha (300 × 150 m). It was assumed that it will become the northern part of the AMU Morasko test site. From this time the older part of the test site is its southern part.

## 2. Geology

Sedimentation of the analyzed soils on the test site, in terms of the depth which was covered by the tests, was the result of deglaciation of the Pleistocene ice sheet, especially melting of blocks of dead ice in the span of ~14–13 k years BP to ~10 k years BP [5]. The location of this area in the zone of an end terminal moraine and sandur [6]—see Figure 2, leads to the coexistence of clayey and sandy sediments. The former (the subject of the studies) are represented by the youngest and relatively thick (even up to 15 m) glacial clay of the Poznanian Phase of the Weichselian glaciation of most probably superglacial origin, i.e. coming from washing out of fine and very fine sediments from the surface of the ice sheet. The latter, on the other hand, come in the form of sandur sands with a dominant fine and medium granulation with a small admixture of gravel. Their transport on the foreground of the ice sheet, with a temporary limitation to the outflow of glacial waters with blocks of partially frozen ice, was linked to phases of melting away and flowing on ice clayey material. As a result, it was additionally enriched with a sandy fraction.

The thickness of the sandur sands that cover the analyzed clayey soils rarely exceed 3 m and they usually range from 1 to 2 meters. They generally rise towards the south, analogical to a mild sinking of the surface towards the stream Strumień Różany (left-bank tributary of the Warta river), which flows near the southern border of the test site. The differences in the terrain ordinates between the northern and southern part of the test site amount to around 5 m (from ~100 m a.s.l. in the north, to ~95 m a.s.l in the south). The drilling and cone penetration test profiles performed in the northern part of the test site often do not show sandy sediments on the surface. Such situation also takes place, only pointwise, at the southern border of the site. Such places allowed locating uncovered excavations to the depth of ~2 m, from which samples in the form of monoliths for the strength and compressibility tests were extracted (Figure 1).

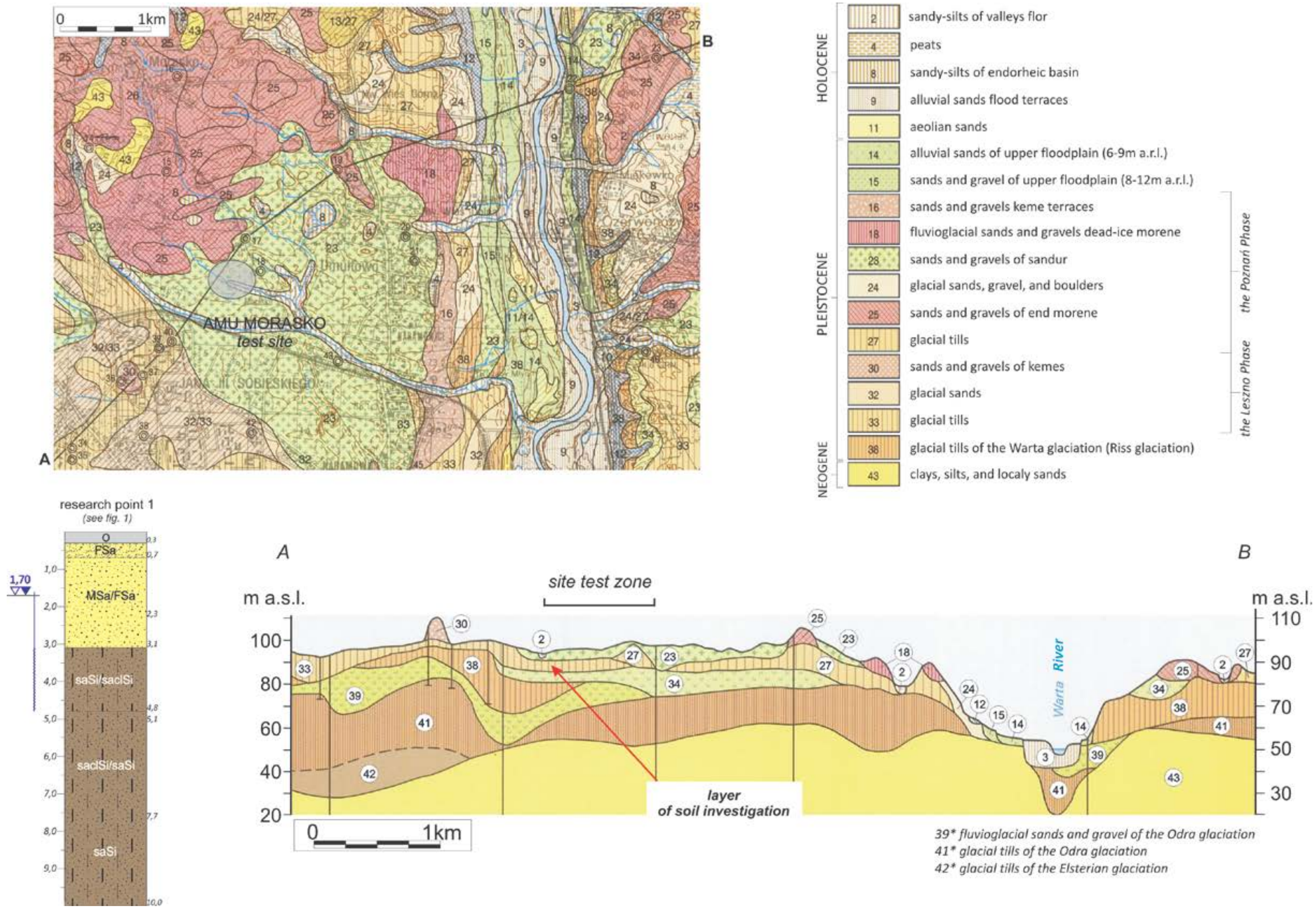


**Figure 2.** Geological structure of the AMU Morasko test site [6] and a typical geological profile of sediments.

Geological structure of the analyzed area is supplemented with sediments which are a latitudinally oriented terminal moraine zone that runs along a curved axis toward the north of the test site with its cumulation on Góra Moraska (154 m a.s.l). The zone is characterized by distorted glaciotectonic glacial till and sandy-gravel sediments from other stages of the Pleistocene glaciations (from Kansan glaciation, through Riss glaciation, to Weichselian glaciation), and also in some areas on the surface, xenoliths of Mio-Pliocene silts of the so-called Poznanian Phase [7]. Creation of the push morain did not significantly affect the strain of the analyzed intermediate soils from the test site because of their deposition most likely in the declining stage of the glaciation and even during deglaciation in the marginal zone of the ice sheet.

Total thickness of the sediments of the quaternary area of AMU Morasko test site ranges between 40 and 60 m, and their lateral and spatial location was designed synthecially within the scope of the Poznań worksheet of a serial geological map of Poland [6] (Figure 2).

A sample and typical geological profile which represents the southern part of the test site (no. 1, Figure 1) is presented by Figure 2. Other profiles—cone penetration tests that present geological structure in detail, which is presented in this chapter, suplement figures in later parts of the text. It is emphasized that the layer of intermediate soils [8], which the presented studies focus on, amount to c. 12 m in both parts of the test site. Moreover, the bottom of the layer has been reported to be present at the depth of : ~15 m (in the southern part of the test site—CPTU S5*) and ~12 m (in the northern part of the test site—CPTU: 1* ÷ 4*). This fact, in connection to terrain's morphology, indicates collapsing of the analyzed layer towards the south, which translates well into the morphogenesis of the whole push moraine of Góra Moraska.

In the presented area, which was analyzed in detail up to 16 m of depth, there is one water-bearing level. It is connected to the surface level of the sandy sediments (sandur). The depth at which the free water table of this level is retained, assessed in May of 2014 for the southern part of the test site, amounted to 1.00 ÷ 2.50 m below the ground level. This corresponds to the ordinate: 92–93.5 m a.s.l. At the same time, the existence of significant water filtration within clayey sediments located under the above-mentioned sands was concluded at the time. The filtration zones were arranged in an irregular manner – forming a mosaic, whereby filtration intensity mildly declined along with the depth. The analysis of the location of the water in: May 2000, in August 2004 and in May 2011 (after a very harsh winter 2010/11) indicates that the determined in 2014 water table corresponds to high levels of uderground waters. It has been proven by further observations, until 2018, where it is currently at least 1–1.5 m lower.

In 2014, the water table in the water course flowing dozens of metres afar from the southern part of the site test boundary was located at the ordinate of c.90 m a.s.l, which should be considered as an axproximate ordinate of a local drainage base in the analyzed area.

## 3. Material composition

### *3.1. Granulation*

Grain size distribution of tens of B category samples according to [9] (of natural granulation and moisture) of an intermediate soil from the AMU Morasko test site, determined using the aerometric method is presented by Figure 3. Part A illustrates synthetic variability of content of basic granulometric fractions in the vertical profile. Part B illustrates representative cumulative curves of grain size distribution based on which the analyzed soils were classified according to [10] as type saSi close to saclSi soils. This case also shows samples extracted from various depths.

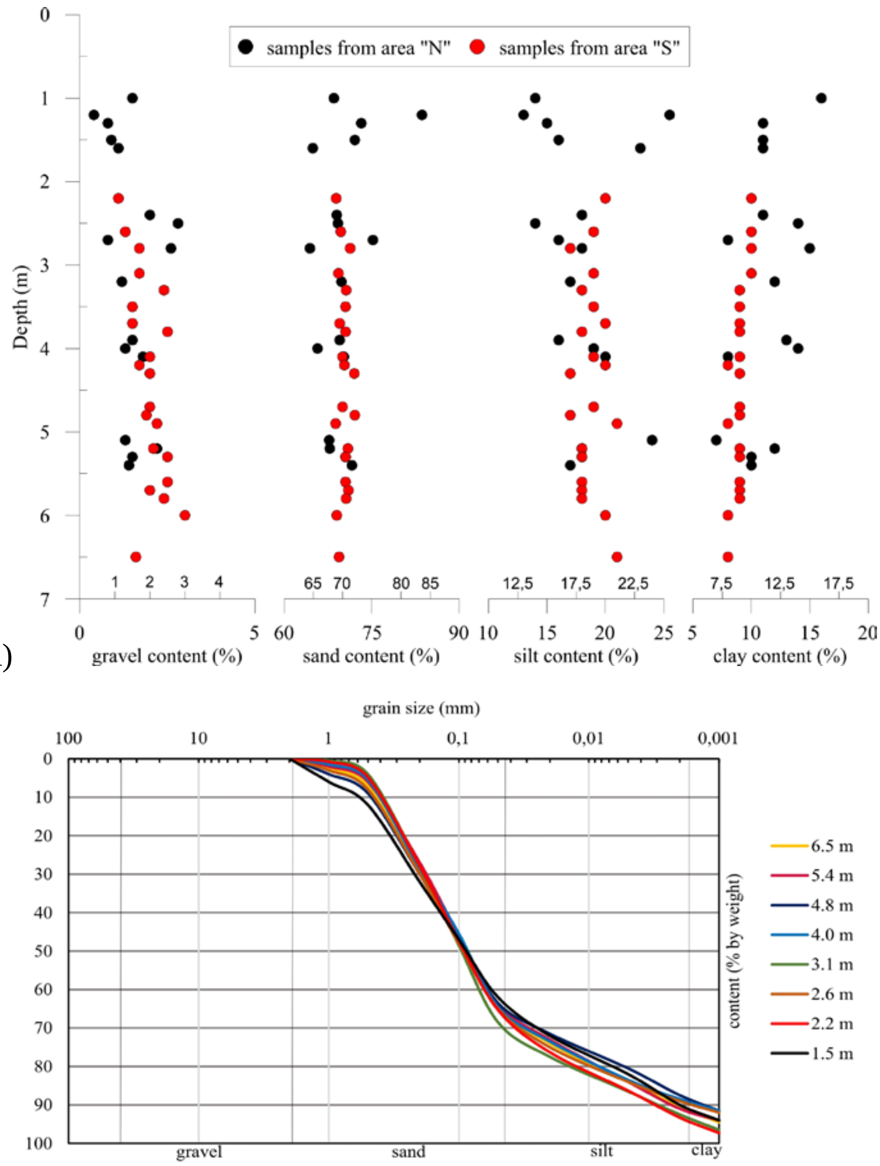


A)

B)

**Figure 3.** Grain size distribution of the intermediate soils at the AMU Morasko test site. A) reference synthesis of measurements B) cumulative curves of grain size distribution of representative soil samples with reference to the depth at which they were extracted.

The content of the silt fraction ranges between 8 and 15% while most of the represented sample contents varies between about 9 and 12%. A greater dispersion of grain size distribution was observed on samples extracted from the northern part of the test site. In surface part of the—profile (up to about 4 m) soil shows a relatively higher content of silt (extremely even up to 18%). The content of dust, sandy and gravel fraction which were extracted from both parts of the test site is comparable and respectively is as follows: 20, 70 and 2%.

### 3.2. Mineral composition and structure

Detailed tests performed on the mineral composition and structural features in the SEM scanning microscopy are being implemented. One of the first tests is depicted by a photograph in Figure 4. With visible quartz, calcite and feldspar grains in clayey matrix built from silty minerals. This figure confirms macroscope observations in the mentioned scope, especially the fact that quartz grains and single gravel grains present in the analyzed soils are characterized by mild mechanical processing, as compared to the average process. They can be classified after Pettijohn [11] as semi-sharpedged grains. Using the gas-measuring laboratory method according to Scheibler only the content of $CaCO_3$ was determined. The results of this study are presented in Figure 5.

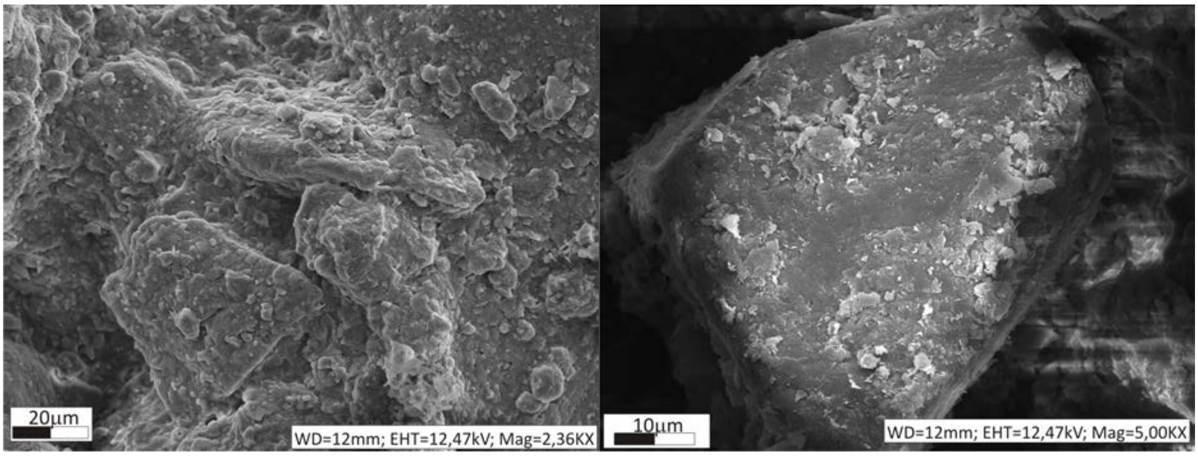


**Figure 4.** The SEM image of the intermediate soil sample (4/5.0 m) from the northern part of the test site at the depth 5 m above the ground surface (left) and single quartz grain with clays minerals on surface (right).

The analyzed soil, in terms of its depth up to 5 m, contains $CaCO_3$. Its content is similar in individual samples, regardless of depth at which they were extracted. Calcium carbonate is present in the profile in a dispersed form. Only in the near-surface zone, up to c. 1.5 m, its accumulation in form of concretion was observed in some places with a diameter of c. 1.5–2 cm.

The structure of the analyzed soil in the macroscopic image is homogenous, massive. Laminations were not found. Because of the presence of filtration zone of groundwater in the subsoil which were signaled earlier, and also considering the characteristics of variability of the recorded CPTU values: cone resistance $q_c$, pore water pressure $u_2$, at the current stage of research it cannot be excluded that this is the result of microstructural features of the analyzed soils. Sample image of very stable $q_c$ values, which can be seen in Figures 6 and 7 with a simultaneous dynamically changing pore water pressure distribution $u_2$ in the subsoil, which amplifies particularly in case of a four times slower cone penetration testing, as compared to the standard velocity, can indicate the presence of small sandy laminas allowing dispersion of the pressure caused by cone penetration. Slower time of this penetration promotes clearer and growing number of zones of declining pressure $u_2$ in the observed profile.

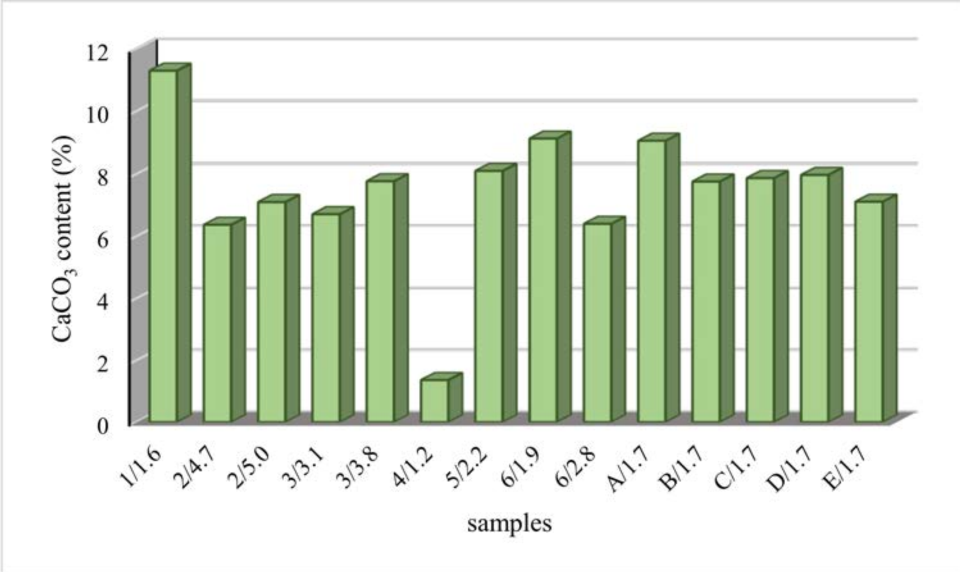


**Figure 5.** The content of $CaCO_3$ in selected samples from intermediate soils (up to the depth of 5 m) from the northern part of the AMU Morasko test site.

As far as this issue is concerned, it is problematic to separate the impact of cone penetration test results on the results of the sand fraction found in the subsoil, which may be present in structurally oriented lamina from the impact of the same fraction, but in a dispersed form in the basic mass of the analyzed soil. Indirectly, this issue is indicated by dissipation diagrams depicted in Figure 8.

Both dissipation tests were performed on analogical depths (4 m), in points located a few hundred meters from each other in the northern and southern part of the test site making sure, prior to the testing process, that the subsoil in this area is cohesive.

Both dissipation curves indicate that pore water pressure reaches the value from before the cone penetration test after less than one hour. This indirectly proves a significant content in the examined layer of the dispersed sand fraction. Horizontal consolidation $c_h$ of the tested soils, calculated for the obtained dissipation curves according to Robertson's formula [12]:

$$c_h = 1.67 \cdot 10^{-6} \cdot 10^{(1-\log t_{50})} \tag{1}$$

where: $t_{50}$—time at 50% dissipation of pore water pressure, reaches similar values: 0.051 cm/s (for S5* test) and 0.057 $cm^2/s$ (for test no. 8).

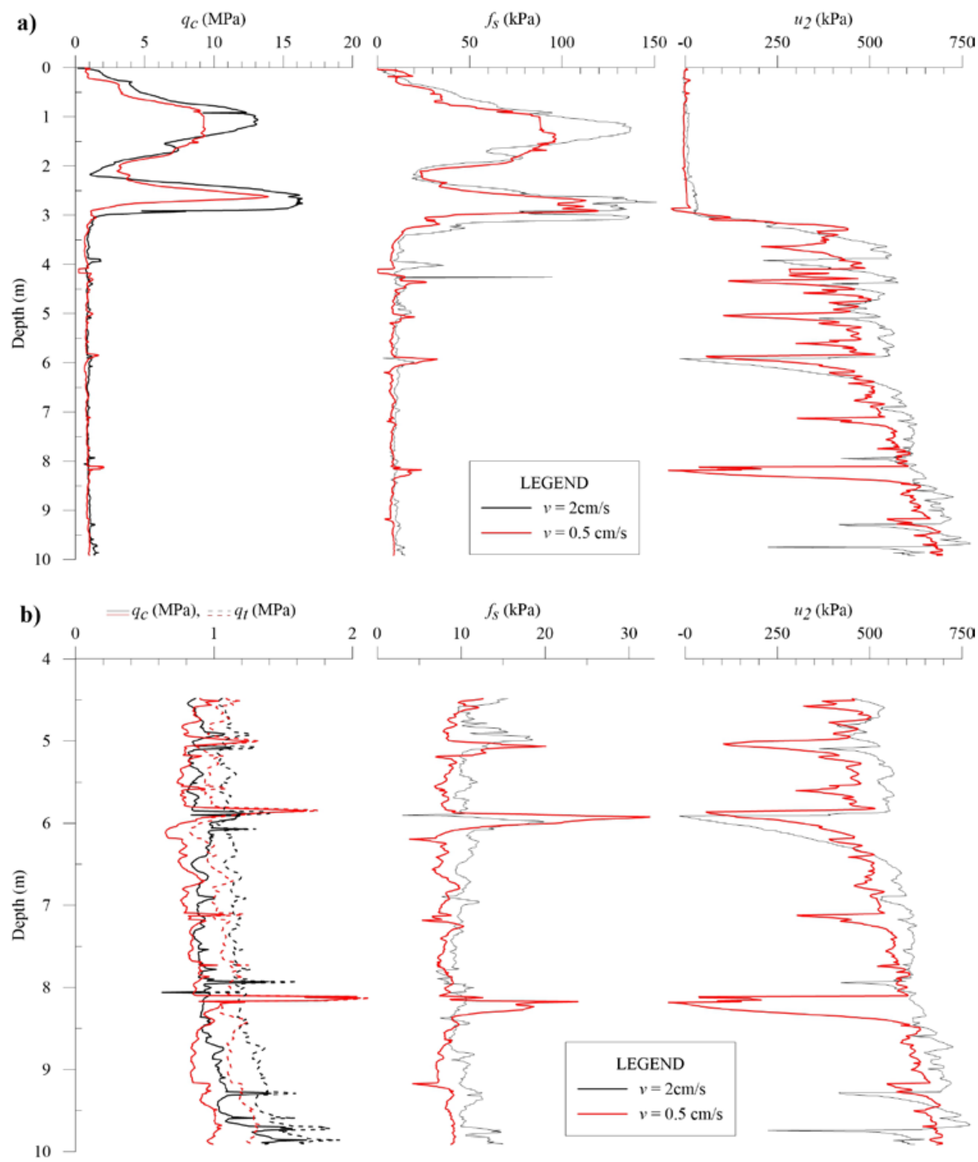


**Figure 6.** Cone penetration test parameters at CPTU S5* (see Figure 1) performed with a standard penetration velocity $v$ = 2 cm/s and $v$ = 0.5 cm/s, along the whole profile (a) and only within the clay layer part (b).

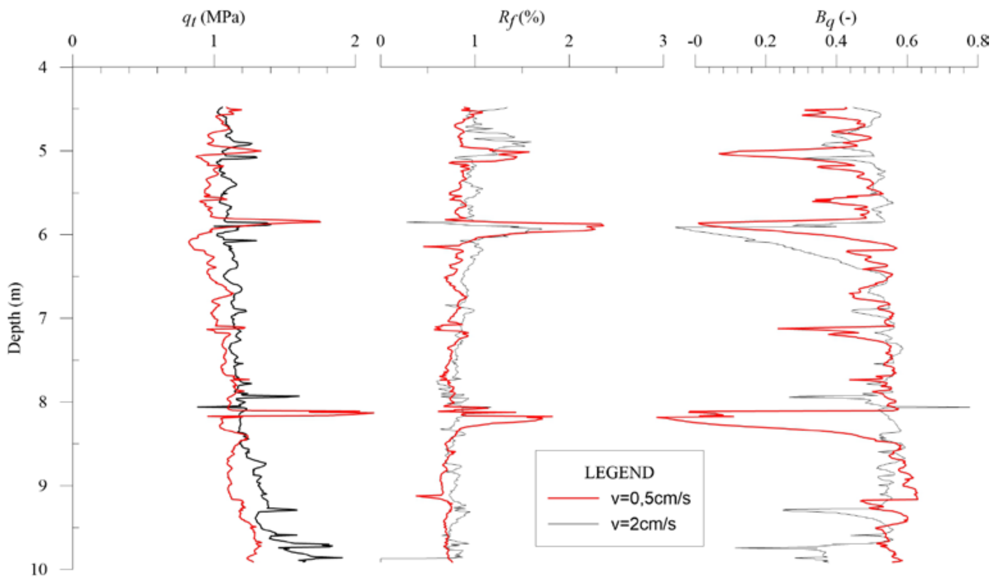


**Figure 7.** The derived parameters: $q_t$ (corrected cone resistance), $R_f$ (friction ratio), $B_q$ (pore pressure parameter), within the clay layer part at CPTU S5*.

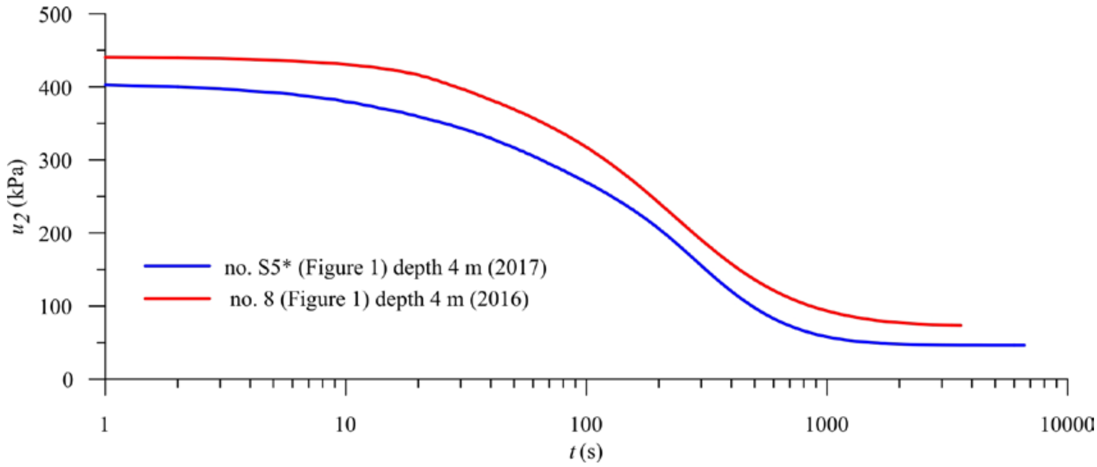


**Figure 8.** The process of pore water pressure dissipation at the depth of 4 m in S5* and 8 (for their location see Figure 1).

## 4. Statistical variability of soil properties

In case of every benchmark test site, its homogeneity, in terms of geotechnical properties, is a significant issue. Regardless of the analysis of variability for the values of individual soil parameters, a good and universal indicator of homogeneity may be the analysis of the values for statistical cone penetration tests. At the AMU Morasko test site such analysis was conducted based on 9 CPTUs performed in different locations using devices from the same manufacturer [13]. These tests were used to analyze differences between: corrected cone resistance—$q_t$, sleeve friction—$f_s$, pore pressure behind cone—$u_2$, friction ratio—$R_f$, soil behavior index—$I_c$, pore pressure parameter—$B_q$ and normalized cone resistance—$Q_t$. The comparison of the results form one cone penetration test to the reference sample consisting of the remaining 8 tests, let to conclude a satisfactory repetitiveness of the results obtained at the test site, below 4 m in particular (Figure 9).

The conducted cluster analysis indicates that, with around 90% of certainty, the layer between 4 and 10 metros of depth can be considered as homogeneous on the entire area of research.

Considering the results obtained by Wierzbicki et al. [13], the performed analyses presented in the next parts of the research paper use averaged statistical cone penetration test results.

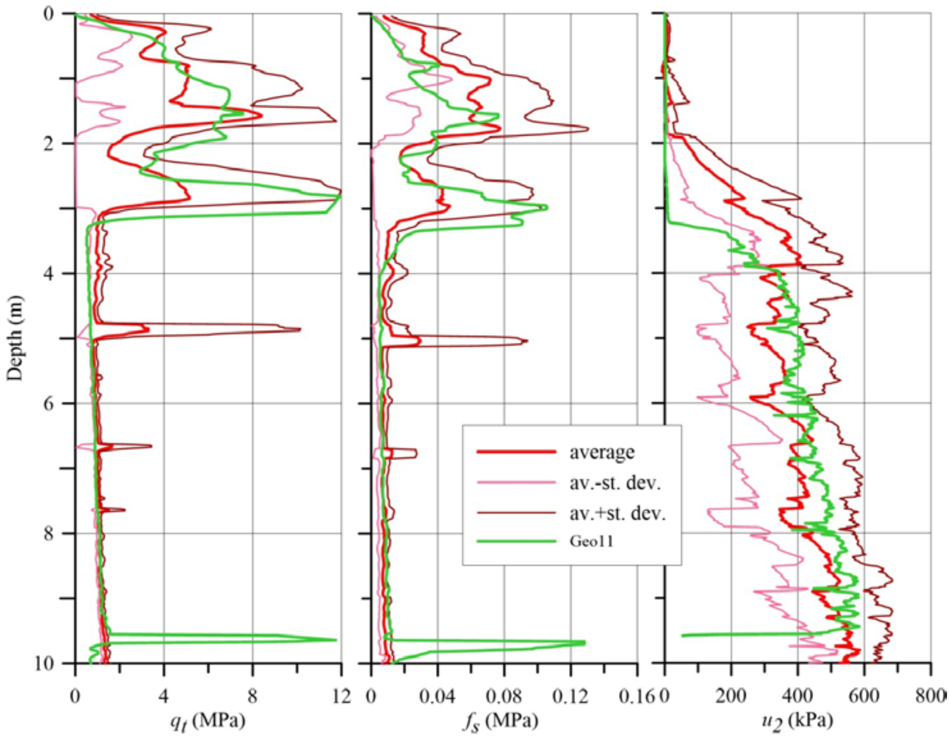


**Figure 9.** The $q_t$, $f_s$ and $u_2$ at reference testing point Geo11 on the background of average values and standard deviation intervals calculated for statistical population of 8 another CPTUs (after [13]).

## 5. State and index parameters

### *5.1. Natural water content and Atterberg limits*

#### 5.1.1. Natural water content ($w_n$)

The values of natural water content of intermediate soils of the test site at AMU Morasko, analyzed as a whole (for N a S parts), are shown by Figure 10. From such a perspective, water content is diversified between 13 and 20 %, which is a relatively broad scope of variability. However, division into samples representing the northern and southern part of the test site is clearly noticeable. The concluded discrepancy is most probably the result of a higher, even 5–6%, silty fraction in soil samples extracted from the northern part of the test site (see Figure 3A). It is worth mentioning that the time period between testing this parameter was three years and natural water conditions in the subsoil may have changed. This fact has been already mentioned while discussing hydrogeological conditions analysis. After separating the results from both parts of the test site, water content of natural samples extracted from the southern part are significantly more convergent in the entire analyzed profile. Their water content amounts to 13.5 ÷ 15%. The samples from the northern part still indicate a vast dispersion of the values $w_n$: 16 ÷ 20%.

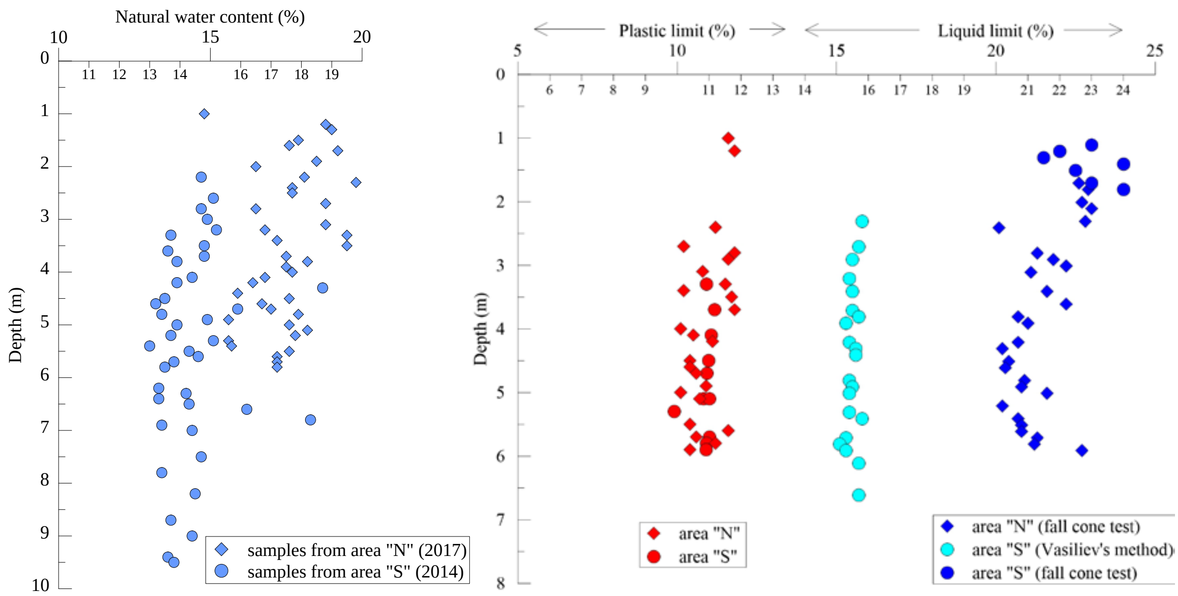


**Figure 10.** Natural water content and Atterberg's limits of intermediate soils at the AMU Morasko test site.

### 5.1.2. Plastic limit (*PL*)

The value of the plastic limit is determined by a rolling method and ranges between 10 ÷ 12%. It is significantly more stable in the soils from the southern part of the test site where it amounts to 11%. It is worth mentioning that the analysis used the results of tests that were conducted independently from each other by several individuals. This, with a relatively high subjectivity of the rolling method, makes the obtained and repetitive result trustworthy. In case of the analyzed soils, subjectivity of the rolling method is even greater because they signify low plasticity. Thus, the rolling attempt itself becomes problematic since the soil reaches the plastic limit and starts to disintegrate.

### 5.1.3. Liquid limit *(LL)*

The liquid limit was determined using two methods: Vasiliev's cone and fall cone. Both methods are based on similar general assumptions (inter alia [14–17]). They determine water content while cone's measurement tip penetrates the soil deeper at a particular depth. However, there are significant differences between these methods in terms of the scope of the marking procedures and some parameters related to the used equipment. Thus, as a consequence, determined results differ as well, which was described by [18,19] respectively indicating the correlation Eqs 2 and 3:

$$LL_{(f.c).} = 1.21 LL_{(Vasiliev)} \tag{2}$$

$$LL_{(f.c).} = 1.29 LL_{(Vasiliev)} - 5.04 \tag{3}$$

Because of specific properties of the analyzed soils, determining *LL* with the Casagrande method was discontinued. It is related to the possibility of easy liquefaction during the examination of soils classified by low plasticity, particularly the ones that contain a significant admixture of dust fraction by creating shear strain generated as a result of striking of the soil located in the container of the Casagrande apparatus against a rubber (elastic) base.

The characteristic of the used equipment and the most significant technical procedures are presented in Table 2.

**Table 2.** Basic characteristics in the method used to examine the liquid limit.

| Parameter | Unit | Vasiliev Cone method | Fall Cone method |
|---|---|---|---|
| Cone angle | (°) | 30 | 30 |
| Cone weight | (g) | 76 | 80 |
| Penetration time | (s) | 5 | 5 |
| Immersion | (mm) | 8–12 | 12–20 |
| Number of replications | (-) | 2 | 4 |

Except for the difference in mass of the incorporated cones, the procedure used to determine the values of the liquid limit were considerably different. As far as the Vasiliev's method is concerned, the *LL* values were considered as water content at the depth of 10 mm where the cone was embedded. As for the cone penetration method, four markings were created and they were used as the basis to create the diagram of correlations of the depth at which the cone was embedded between the water content. On that basis, water content was recorded $w_{18}$ (at the depth of 18 mm), next *LL* was calculated according to the formula (Eq 4) [17,20]:

$$LL = 0.0043 w_{18}^2 + 0.8873 w_{18} + 3.62 \tag{4}$$

Only after the above-mentioned explanations are taken into consideration, it is possible to analyze the results of the liquid limit values, which can be seen in Figure 9.

At the beginning the *LL* test of the sampled extracted from the southern part of the test site was performed only using the Vasiliev's method. However, the samples from the northern part were assessed using the cone penetration test. The discrepancies in *LL* amounting to even 6%, with a simultaneous macroscopically similar to the condition of soils from both parts of the site and with a similar grain size (classifying all the soils as saSi or saclSi) caused the necessity to implement additional tests, which are currently being performed. The initial analyses complementing the methodology of sample testing from the northern part of the site indicate that after implementing the same methodology of marking, i.e. *LL* for the samples extracted from the southern part of the test site (cone penetration method) these values become comparable to the samples obtained during earlier soil samples from the northern part. However, they are c. 30% higher than the values obtained using the Vasiliev's method. At the same time, they are better when it comes to depicting the actual geotechnical condition of the examined soils. This condition, expressed e.g. by the liquidity index (*LI*) , while implementing its calculated values (Eq 5) for the plastic limit determined the with Vasiliev's method usually indicated that the analyzed soils are at between soft and liquified or even liquid state. This was not consistent with the actual values obtained macroscopically. Considering above mentioned facts it should be assumed that the observed discrepancy in the results is logical and only proves statistical correlations obtained by NGI [18] and DeGroot et al. [19].

The intermediate soils from the AMU Morasko test site are characterized by a relatively stable liquid limit in the profile ranging between 20 ÷ 23%. The cone penetration method is recommended for its examination.

### *5.2. Plasticity index (PI) and liquidity index (LI)*

Based on the determined values of Atterberg's limit, the plasticity index of the tested soils was determined. For this purpose, the liquid limit was implemented and calculated with the fall cone method. Regardless of remarks presented in chapter 5.1 about the test methodology, it can be observed that *PI* values correspond really well to the percentage content of the silty fraction in the analyzed soils and typical *PI* values observed in the soils of similar origin on the territory of Poland [21] (Figure 11).

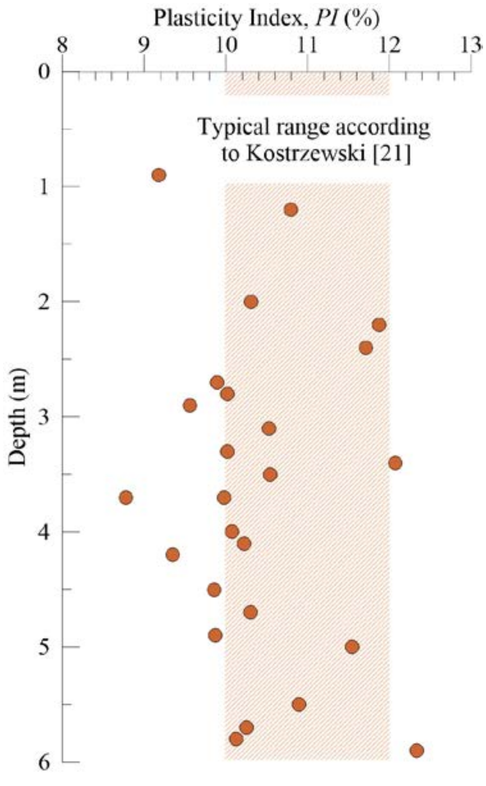


**Figure 11.** Changes in the values of the plasticity index (*PI*) in the AMU test site profile.

The character of tests conducted on geotechnical properties of the soils in Poland resulted in the fact that for many years prior to the introduction of the Eurocode and ISO standards, the main parameter characterizing cohesive soils was liqiudity index (Eq 5).

$$LI = \frac{w_n - PL}{LL - PL} \tag{5}$$

In spite of actual changes in the form of examining the properties of geotechnical soils, it is still one of the main parameters whose values are determined in practice. Thus, the Polish literature contains many formulas which enable determining the *LI* values, e.g. based on CPTU results. The *LI* values of the examined soils obtained with a set of selected calculation methods based on laboratory analyses are presented in Figure 12. For the purpose of these calculations particular formulas, which also took into consideration the class of the examined soils, created by Młynarek et al. [22] (Eq 6) and Liszkowski et al. [23] (Eqs 6, 7 and 8) were implemented

$$LI = 0.517 q_n^{-1.44} \text{, for last glaciation tills with } PI\text{=10 ÷ 30} \tag{6}$$

$$LI = 0.31 - 0.26 \ln(q_n) \text{, for last glaciation tills with } PI\text{=20 ÷ 30} \tag{7}$$

$$LI = 0.5 - 0.33 \ln(q_n) \text{, for last glaciation tills with } PI\text{=10 ÷ 20} \tag{8}$$

where: $q_n$—net cone resistance from CPTU in MPa.

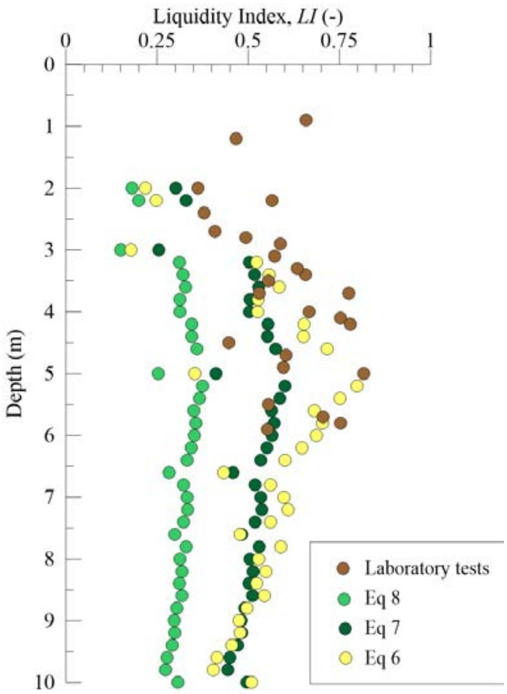


**Figure 12.** Liquidity index (*LI*) of the AMU test site soils determined with various methods.

According to earlier predictions, the *LI* values determined using Eq 8, predicted for the use in case of glacial tills of higher plasticity, mostly diverge from the laboratory test results The two remaining formulas (Eqs 6 and 7) satisfactorily resemble real *LI* values. In general, the consistency of soils that can be found at the AMU test site is plastic in the top part of the profile in order to become soft-plastic in the lower parts and again becoming plastic in the deeper parts of the profile.

*5.3. Soil unit weight ($\gamma$)*

One of the basic parameters characterizing the soil is its density ($\rho$). This parameter is a starting point for most of geotechnical analyses and it allows calculating the soil unit weight and, in accordance with superposition, the *in situ* vertical stress $\sigma_{v0}$ values. The laboratory determination of the soil unit weight may be a significant challenge, especially if saturated intermediate soils are examined, where undisturbed sample is problematic. In the Polish geotechnical practice, in order to determine an initial unit weight and a unit weight of soil particle ($\gamma_s$) a tabular overview from the Polish standard [24] is usually used. The authors of this report assumed that the soil unit weight is a derivative of a mineralogical composition, grain size distribution, natural water content and geological track record of soil. Therefore, considering the specifics of cohesive soils found in Poland, the soil unit weight depends on grain size distribution and the liquid index. The accuracy of the information presented in these overviews, especially in terms of glacial tills was confirmed multiple times [25]. Hence, as a reference value of the soil unit weight found at the AMU test site, the values determined based on [24] were adopted. Additionally the values of unit weight were calculated on the basis of Eq 9, assuming the soil was fully saturated.

$$\gamma = \frac{(G_s + e)\gamma_w}{1 + e} \tag{9}$$

where: $\gamma$—soil unit weight, $\gamma_w$—water unit weight kN/m$^3$, $e$—void ratio calculated on the basis of $w_n$ form Figure 10, $G_s = \gamma_s/\gamma_w$ and $\gamma_s$ was assumed from [24] equal to 2.65.

The results of the measurement points of the soil unit weight performed on intact samples and overview of the soil unit weight determined based on CPTU (Figure 13) were presented against the aforementioned background. For this purpose, three formulas were adopted. Two of them are well known in the worldwide literature: Robertson [26] (Eq 10) and Mayne [27] (Eq 11) and one developed for glacial tills for the western part of Poland by Lasowska [25] (Eq 12):

$$\frac{\gamma}{\gamma_w} = 10\left(0.27\log R_f + 0.36\log\frac{q_t}{p_a} + 1.236\right) \tag{10}$$

where: $\gamma$—soil unit weight, $\gamma_w$—water unit weight kN/m$^3$, $R_f$—CPTU friction ratio, $q_t$—CPTU corrected cone resistance in kPa, $p_a$—atmospheric pressure,

$$\gamma = 26 - \frac{14}{1 + \left(0.5\log(f_s + 1)\right)^2} \tag{11}$$

where: $\gamma$—soil unit weight, $z$—depth in m, $f_s$—CPTU sleeve friction in kPa, $q_t$—CPTU corrected cone resistance in kPa,

$$\gamma = 23.64 - \frac{4.1}{1+\left(0.5\log\left(f_s+1\right)\right)^2} \tag{12}$$

where: $\gamma$—soil unit weight, $z$—depth in m, $f_s$—CPTU sleeve friction kPa.

Observation of the data presented in Figure 13 allows to notice a large discrepancy between the results of Eqs 10 and 11 and values determined based on the Polish norm and Eqs 9 and 12. The discrepancy amount to 20% and can turn out to be significant in evaluating vertical stress values. It also is noteworthy to notice that in case use of Equation 9, the influence of precise measurements of natural water content is significant. For example, the difference of 3% of moisture (as can be seen at Figure 10) causes in difference of 1 kN/m$^3$ in soil unit weight. In this case the calculations of soil unit weight needs also a high quality samples, protected by the draining out the water during the recovery.

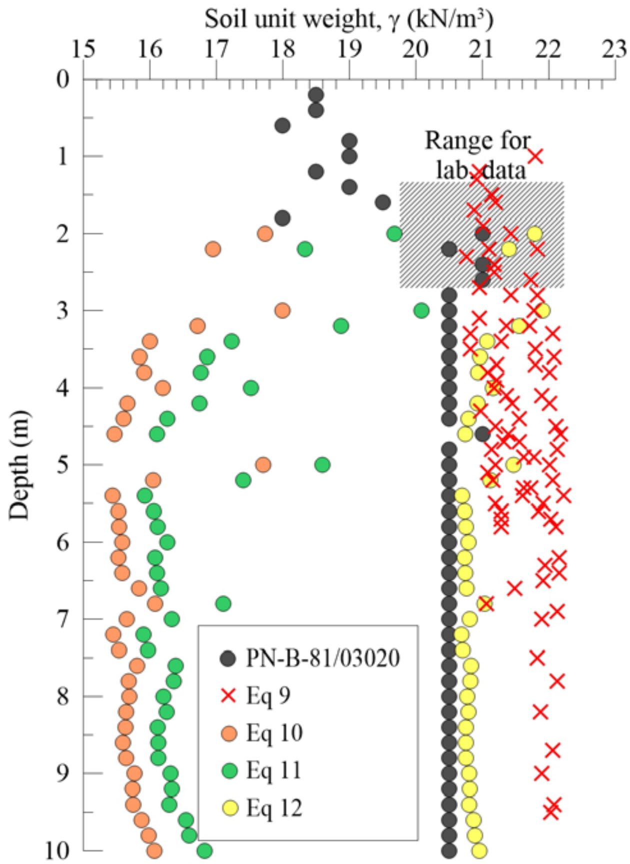


**Figure 13.** An overview of the soil unit weight values at the AMU test site determined using various methods

*5.4. In situ stresses and stress history*

One of the important features of a subsoil is its geostatic stress state. The geostatic stresses can be modified by the preconsolidation processes, which can yield the overconsolidation effect. This effect can be quantified by the overconsolidation ratio (OCR). The values of OCR on the test site were determined using in situ test results. In case of DMT the equations were as follows: Marchetti [28] (Eq 13) and Lunne et al. [29] (Eq 14), however, in case of CPTU the following equations were implemented: Wierzbicki [4] (Eq 15), Karslrud et al. [30] (Eq 16), Kulhawy and Mayne [31] (Eq 17) and Robertson [26] (Eq 18).

$$OCR = 0.K_D{}^{1,56} \tag{13}$$

$$OCR = 0.3K_D{}^{1,17} \tag{14}$$

$$OCR = 5.25 \ln Q_t - 14.97 \text{, for } PI\text{=10÷20} \tag{15}$$

where: $Q_t$—CPTU normalized cone resistance.

$$OCR = \left(\frac{Q_t}{3}\right)^{1,2} \tag{16}$$

$$OCR = kQ_t \tag{17}$$

where: $k$ = 0.2 (for young clays).

$$OCR = 0{,}25Q_t^{1.25} \tag{18}$$

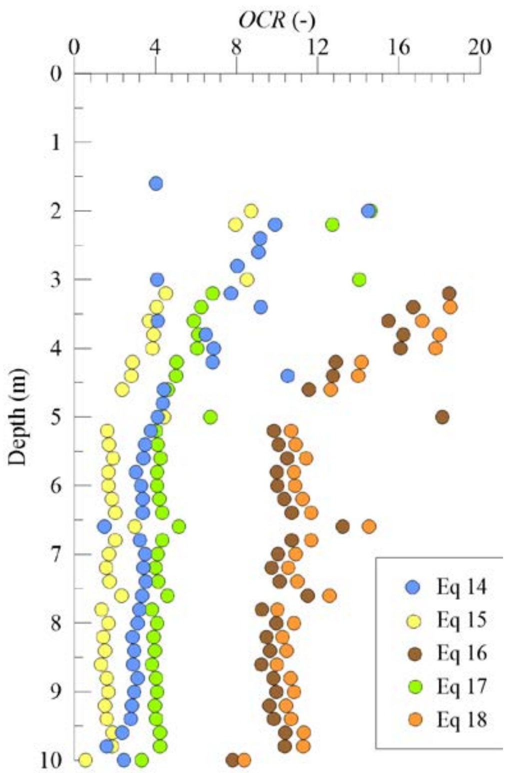


**Figure 14.** *OCR* values of AMU test site soils, determined with various methods.

Among all the obtained results, a strong tendency to a clear decrease in the *OCR* value in the top part of the profile draws attention (Figure 14). In the context of geological studies, the cause of this effect can be both the influence of overflow pressure during the creation of fluvioglacial sand layers, as well as the observed carbonate cementation in this zone. Regardless of this claim, it can be assumed that *OCR* values above, obtained based on some of the methods, do not reflect the actual state in normally consolidated soils.

Considering local experience, verified by partial laboratory test results to calculate the values of in situ vertical stress, the values of soil unit weight were implemented determined based on the Polish standard. Determining *in situ* vertical effective stress $\sigma'_{v0}$ and *in situ* horizontal effective stress $\sigma'_{h0}$ required taking into consideration the ground water content in the analyzed profile and, in the second case, determining the coefficient of earth pressure at rest ($K_0$) (Figure 15). In order to calculate in situ effective horizontal stress, the coefficient of earth pressure at rest was calculated based on DMT, according to the Lunne et al. [29] (Eq 19).

$$K_0 = 0.34 K_D^{0.54}\text{, for young clays} \tag{19}$$

where: $K_D$—DMT horizontal stress index.

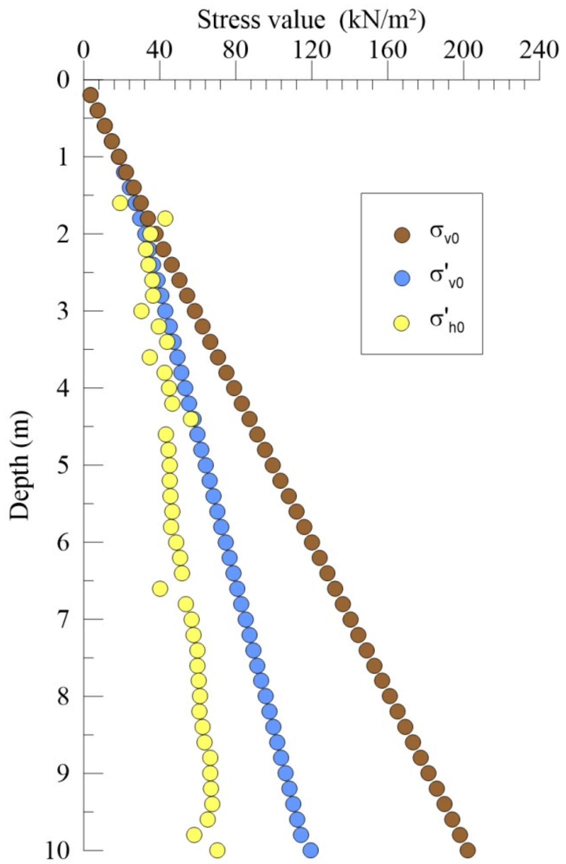


**Figure 15.** Distribution of in situ stresses values in the AMU test site profile.

The $K_0$ values determined according to Equation 19, can be treated in this case as some kind of reference point considering a verified applicability of the formula in moraine soils [4]. The computed

$K_0$ values will depend on the correlations used and can vary with a factor of 2. In order to illustrate this issue, $K_0$ values for the AMU test site were calculated with different methods, and obtained results were presented in Figure 16. Kulhawy and Mayne's formula [31] (Eq 20) and Marchetti's formula [28] (Eq 21) were used for the calculations

$$K_0 = 0.428 OCR^{0.414} \tag{20}$$

where: $OCR$—overconsolidation ratio, calculated on the basis of CPTU results and Eqs 15, 16, 17 and 18.

$$K_0 = \left(\frac{K_D}{1.5}\right)^{0.47} - 0.6 \tag{21}$$

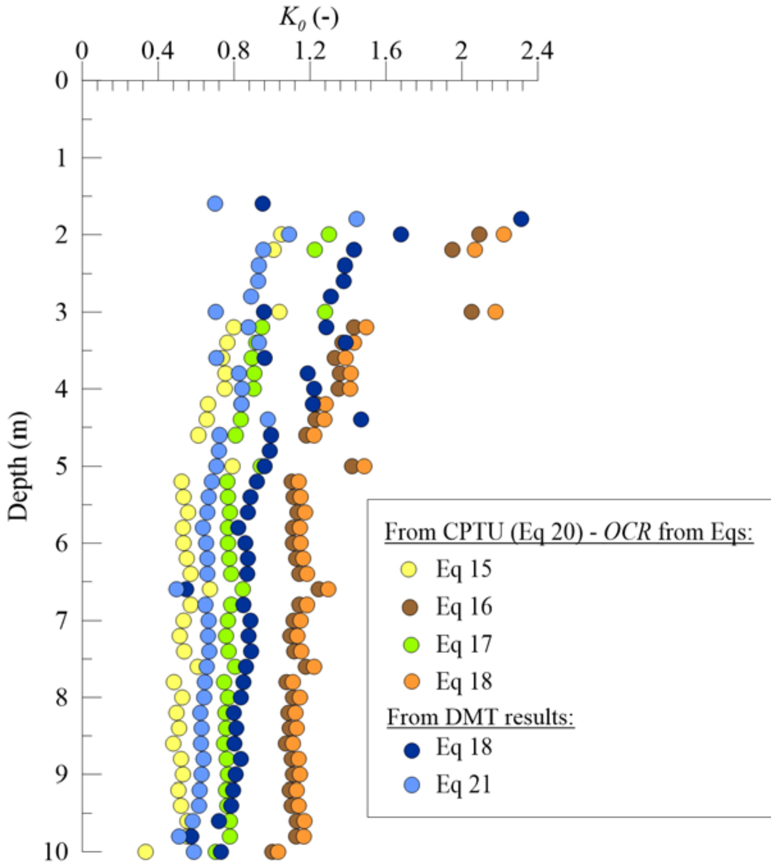


**Figure 16.** $K_0$ values in the profile at the AMU test site, determined with various methods.

As pointed in chapter 1, the geological analysis of the area clearly indicates the lack of mechanical preconsolidation of the analyzed sediments. Considering this fact, it can be assumed that calculation results obtained using Lunne et al. [29] (Eq 19) and Kulhawy and Mayne [31] (Eq 20) methods and using Wierzbicki's equation [4] (Eq 15) produce the most realistic results.

It should be borne in mind that many of the correlations are based on clays that are quite different to the AMU site clay, hence the predicted $K_0$ and *OCR* values are associated with considerable uncertainties.

## 6. Engineering properties

### *6.1. Soil compressibility*

Compressibility of the analyzed soils was assessed by determining constrained modulus (*M*) values. For this purpose an oedometric IL test on intact samples and in situ test results were used. Because of the lack of samples of intact structure form deeper parts of the profiles, IL tests were limited only to the top part of the subsoil (c. 2 m deep). The analyses were conducted using a 24-hour method in terms of stress 0–400 kPa. To check a possible anisotropy of deformation properties of the AMU soft in this zone, samples were examined in the horizontal (natural) and vertical positioning.

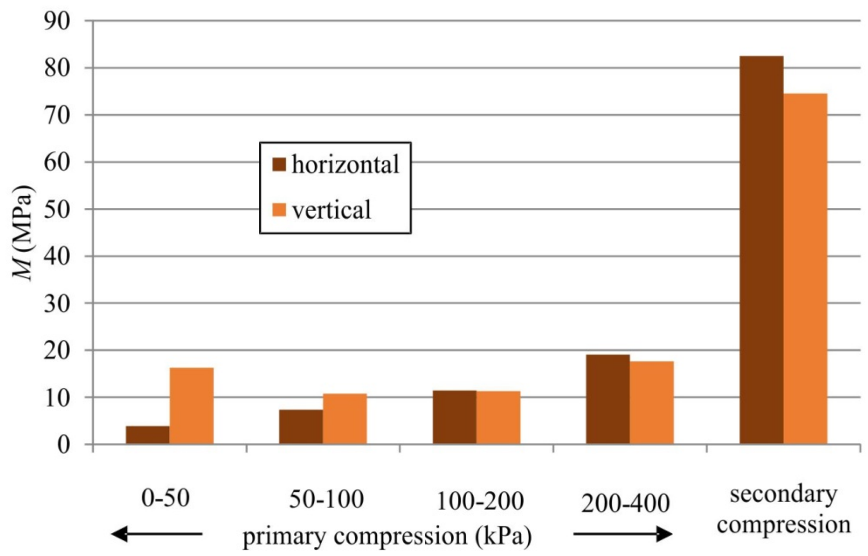


**Figure 17.** *M* values of soils from the AMU test site, determined in IL, in different ranges of strain (secondary compression for range 200–400 kPa).

The analysis of average values *M* in particular ranges of load clearly indicates that some anisotropy can be noticed only within a range of a mild load, up to 100 kPa (Figure 17). This effect can be a result of the presence of the aforementioned small preconsolidation effect, supported with weak carbonate cementation whose impact fades away at greater load values. On the other hand, the thesis about normally consolidated character of the analyzed soils differs four times when it comes to the initial and secondary compressibility modulus (determined within the range of 200–400 kPa).

Average *M* values determined in the oedoemetric study, although fragmented, fit into the general range of the values of this parameter based on the in situ test (Figure 18). To determine the value of *M* based on CPTU formulas by Kulhawy and Mayne [31] (Eq 22) and Młynarek et al. [32] (Eq 23), and the DMT Marchetti's formula [28] (Eq 24).

$$M = 8.25(q_t - \sigma_{v0}) \tag{22}$$

$$M = 13.13(q_t - \sigma_{v0}) \tag{23}$$

$$M = E_D R_M \tag{24}$$

where: $E_D$—dilatometer modulus, $R_M$—correction factor according to Marchetti [28].

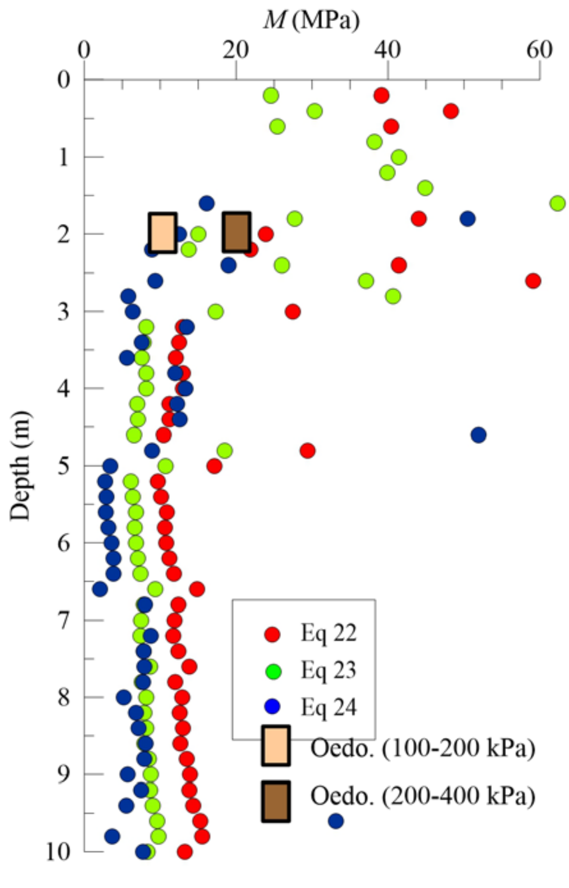


**Figure 18.** *M* values in the profile from the AMU test site, determined with CPTU and DMT and during oedometric tests.

Based on the obtained results it can be noticed that though *M* values calculated based on Eqs 22 and 24 correspond to the load range of 100–200 kPa, based on Eq 23 characterize well soil properties in higher ranges of load.

## *6.2. Small strain stiffness*

The stiffness of the subsoil in terms of small deformations was determined based on the measurement of the shearing wave velocity ($v_s$). The test was performed using the down hole method, with a SDMT seismic measurement model. Based on these measurements using Eq 25 and soil unit weight determined as presented in chapter 5.1, small shear strain modulus ($G_0$) values were calculated. For the comparison to the measured values, the values determined based on CPTU and correlations suggested by Młynarek et al. [33] for overconsolidated glacial tills (Eq 26) were juxtaposed.

$$G_0 = \rho^2 v_s \tag{25}$$

$$G_0 = 361 - 323.23LI - 0.323\sigma'_{v0} - 0.125\sigma'_p \tag{26}$$

where: *LI* from Eq 6, $'_p$—preconsolidation pressure (may be calculated using $'_{v0}$ and Eq 15), note that $G_0$, $'_{v0}$ and $'_p$ should be in the same units.

As Figure 19 shows, the measured $G_0$ values change in the profile of the examined sediments within small limits, indicating a mild increasing trend the deeper they are found. It is worth mentioning that the values, measured based on CPTU differ from the ones determined during direct research to a minor extent retaining a cohesive trend in their alterations.

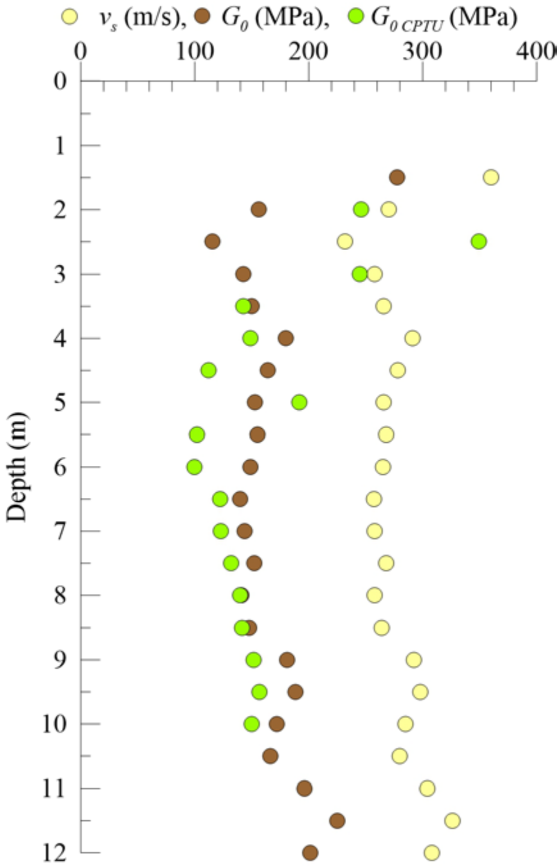


**Figure 19.** Shear wave velocity ($v_s$) value and small shear strength modulus determined based seismic tests ($G_0$) and CPTU ($G_{0\,CPTU}$), in the profile of sediments at AMU test site.

### *6.3. Undrained shear strength ($s_u$, $c_u$)*

Undrained shear strength is a basic parameter that characterizes cohesive soil in terms of strength. In case of intermediate soils, a significant aspect of the analysis of this feature is the velocity at which the test is conducted and pore water pressure dissipation possibilities related to the velocity [34]. As it was pointed in chapter 3, analyzed soils are characterized by good (as for cohesive soils) filtration properties. The influence of rate effect on obtained results, which were determined during the analysis of the AMU soft clay with direct shear box apparatus (DS) and modifying penetration velocity during cone penetration testing. In case of the DS test results reproduced samples were tested, trying to achieve the condition of soil close to its natural form. The test result showed a clear correlation between the test rate and strength properties, which particularly in case of friction angle, is of logarithmic function in nature (Figure 20).

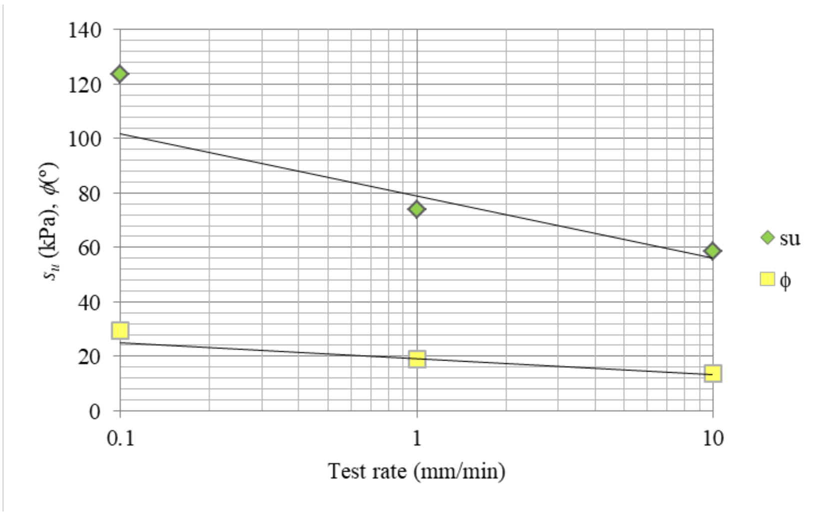


**Figure 20.** Correlation between the values of $s_u$ and $\phi$ and shearing rate in DS test on reproduced samples.

In contrast, Figures 6 and 7 shows the influence of cone penetration velocity reduction as significant in terms of pore water pressure measurements $u_2$. In the soft clay layer an insignificant impact of test velocity was also recorded for the friction measurement (side wall) $f_s$. However, it is barely visible in case of cone resistance $q_c$, the influence of $u_2$ on calculated $q_t$ values makes that also the assessment of $s_u$ is influenced by the penetration rate.

Undrained shear strength in the *in situ* conditions was determined using three methods: CPTU, DMT and field vane test (FVT). In case of cone penetration test, an established correlation was used (Eq 27), however, taking into consideration different values of cone factor $N_{kt}$. Three different coefficient values were adopted: $N_{kt}$ = 15 (adopted average value for similar soil tests in Poland), $N_{kt}$ = 13 (based on Mayne and Peuchen [35]) and $N_{kt}$ = 8 (based on Stefaniak [36]).

$$s_u = \frac{q_n}{N_{kt}} \tag{27}$$

In case of DMT the Marchetti's formula [28] was implemented (Eq 28).

$$\frac{s_u}{\sigma'_{v0}} = 0.22(0.5K_D)^{1.25} \tag{28}$$

Vane test was conducted using a device with a two-part rod, which prevented taking into account rod friction against the soil during the rotation of the drilling cross. The study was conducted according to [37], using the speed of the drilling cross rotation (5°/min). After reaching the maximal value of rotation resistance, determined resistance was also assessed by rotating the drilling cross 720° during 15s. Shear strength was calculated using Eq 29.

$$s_{u,FVT} = \frac{2T_{\max}}{\pi D_v^2\left(H_v + \frac{D_v}{3}\right)} \tag{29}$$

where: $T_{max}$—maximal torque during shearing (kNm), $H_v$ and $D_v$—height and diameter of vane ($H_v/D_v = 2$).

Comparing the obtained results (Figure 21) indicates that both the results of DMT and CPTU (using $N_{kt}$ = 13 or 15) show similar $s_u$ values as well as similar values to the results of replicated samples in the DS apparatus and determined value of this parameter assessed during FVT. On the other hand, considering $N_{kt}$ = 7 causes soil characteristics to be similar to the maximal shear strength value from FVT. It should be noted that the big scatter of the $s_u$ values on the Figure 21, is strongly influenced by the using of different reference values for $N_{kt}$ calculations.

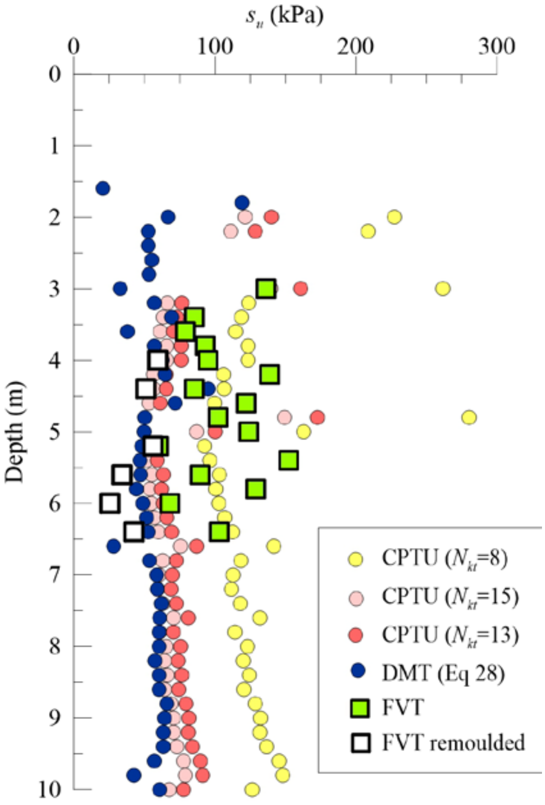


**Figure 21.** The $s_u$ values in the profile from the AMU test site, determined by CPTU, DMT and FVT.

The value of the structural sensitivity coefficient *IR* (Eq 30), determined based on FVT results, ranges from 1.1 to 2.7, showing an increasing tendency along with depth. These values allow to classify the examined soils as low sensitivity (*IR* < 4).

$$IR = \frac{s_u}{s_{u,remoulded}} \tag{30}$$

## 7. Further plans for developing the AMU test site

The upcoming test plans are primarily related to creating in the southern part of the test site core drillings with extraction of high quality undisturbed samples, as well as conducting specialist strength studies in the triaxial shear apparatus and oedometric tests, such as IL and CRS. It is directly related to finalizing plans of the university to build a student dormitory. After its construction the mentioned part of the test site will be excluded from any further soil tests. However, a permanent network of geotechnical monitoring is planned instead, starting from its construction, and mostly at the stage of the building exploitation. This information will allow comparing real behavior of the subsoil with the prognosis resulting from tests on its geoetechnical parameters in the future. Regardless of this fact, lada test made of micropiles will be conducted in these parts of the test site in the following months.

Implementation of other research points is being planned simultaneously to the already mentioned works (core drillings, CPTU, DMT and FVT) in the northern part of the test site. Its goal is successive enlargement of data on the parameters of the analyzed soil to the extent which will enable the use of advanced technology for their statistical processing. As far as this part of the test site is concerned, hole and surface seismic along with conducting electro-resistance profiling are planned.

The very idea of the test site is also enabling comparative studies using different research facilities and sharing knowledge about the soil types and applicability of various testing methods.

## 8. Conclusions

The studies that have been conducted allowed the conclusion that below 4 m in the subsoil there are normally consolidated glacial soils, which can be classified clayey and silty sands. Such soils are often used as a subsoil of constructions in the north-western Poland. Their properties cause difficulties in geotechnical designing in the area where they can be found.

It should be concluded that for typical forms occurrence of such soils the tailings found in the region of the AMU test site are characterized by a uniquely high thickness and relatively high homogeneity. This enables one to use them as a reference test site.

Physical properties of these soils, Atterberg limits and unit weight in particular, have got typical values for such type of soils. The low degree of consolidation and a large content of the sandy fraction results in the fact that these soils are characterized by high compressibility and low, as in case of glacial soils, undrained shear strength. At the same time, a significant fraction of silt proves that they show, typical for intermediate soil, sensitivity to test rate.

The performer studies show that for such type of soils, typical correlations used to for interpretation of the in situ tests have got a limited applicability. Local solutions, however, proved their usefulness. The solutions were designed for soils formed during the Weichselian glaciation. Such conclusion, yet again, proves a limited universality of interpretation methods of the in situ tests indicating that constructing local test sites, such as the AMU test site, is legitimate.


## Acknowledgements

The authors of this research paper would like to thank the authorities of Adam Mickiewicz University in Poznan for the possibility of locating the test site on the territory of the University campus of Morasko and creating convenient conditions that allowed the implementation of the research.

The group of students from the Institute of Geology UAM in Poznanian also deserve a special recognition for the possibility of using their test results in this paper which were conducted on the test site within the scope for the purpose of their thesis papers (engineering and masters theses).

A special acknowledgement is also well deserved to individuals supervising the project GEOCENTRUM DOSKONAŁOŚCI no. POWR.03.01.00-00-K187/15, financed from the UE funds, for financing and enabling and conducting in 2016 and 2017 on the test site a training for students about the operating the cone used for penetration tests. These test results provided analitycal material and significantly enriched knowledge about the described test site.


## Conflicts of interest

All authors declare no conflicts of interest in this paper.

## References


1. Włodarski W, Papis J, Szczuciński W (2017) Morphology of the Morasko crater field (western Poland): Influences of pre-impact topography, meteoroid impact processes, and post-impact alterations. *Geomorphology* 295: 586–597.
2. Karczewski A (1976) Morphology and lithology of closen de-pression area lockated on the north slope of Morasko Hill near Poznań. In: Hurnik H, editor. *Meteorite Morasko and region of its fall*, Poznań, Poland: Wydawnictwo Naukowe UAM, 7–19.
3. Stankowski W (2008) Morasko Meteorite. A curiosity of the Poznań region: Wydawnictwo Naukowe UAM Poznań, Poland, 94.
4. Wierzbicki J (2010) Evaluation of subsoil overconsolidation by means of in situ tests at aspect of its origin: University of Life Sciences in Poznań Publishing, Poland, 182.
5. Stankowski W (2011) Rezerwat Meteoryt Morasko—morfogeneza kosmiczna zagłębień terenu. *Landf Anal* 16: 149–154.
6. Chmal R (1990) Szczegółowa Mapa Geologiczna Polski w skali 1:50000 ark. Poznań (Large-scale Geological Map of Poland, sheet Poznań), Warszawa, Poland: PIG.
7. Chmal R (1997) Objaśnienia do Szczegółowej Mapy Geologicznej Polski w skali 1:50000 ark. Poznań (Explanation for Large-scale Geological Map of Poland, sheet Poznań), Państwowy Instytut Geologiczny, 35.

8. Radaszewski R, Stefaniak K (2017) The problem of determining shear strength of intermediate soils. *Prz Geol* 65: 864–872.
9. ISO (2006) Geotechnical investigation and testing. Sampling methods and groundwater measurements. Part 1: Technical principles for execution.
10. ISO (2017) Geotechnical investigation and testing. Identyfication and classification of soil.
11. Pettijohn FJ (1975) *Sedimentary rocks*, 3 Eds, New York: Harper & Row, 618.
12. Robertson PK (2010) Estimating in-situ soil permeability from CPT & CPTu. 2nd International Symposium on Cone Penetration Testing, Huntington Beach, CA, USA.
13. Wierzbicki J, Radaszewski R, Waliński M (2018) The variability of CPTU results on the AMU-Morasko soft clay test site. In: Hicks MA, Pisano F, Peuchen J, editors, *Cone Penetration Testing 2018*, London: Taylor and Francis Group, 703–708.
14. Farrell E, Schuppener B, Wassing B (1997) ETC 5 Fall-Cone Study. *Ground Eng* 30: 33–36.
15. Hansbo S (1957) A new approach to the determination of the shear strength of clay by the Fall Cone Test. *Proc Royal Swedish Geotechnical Institute* 14: 7–14.
16. Koumoto T, Houlsby GT (2001) Theory and practice of the fall cone test. *Geotechnique* 51: 701–712.
17. PKN (1988) PN-88/B-04481; Grunty budowlane. Badania próbek gruntu (Polish standard PN/B-03020: Building soils. Laboratory test).
18. NGI (2005) Specific correlations between index parameters. Norwegian Geotechnical Institute. 11–20.
19. DeGroot DJ, Landon MM, Metzger SA (2006) Comparison of Russian and Scandinavian Fall Cone Methods for Determining Liquid Limit Using Natural Soils. Amherst: University of Massachusetts Amherst, 1–29.
20. Jaśkiewicz K, Wszędyrówny-Nast M (2013) Wpływ metodyki oznaczania granic Atterberga na uzyskiwane wartości stopnia plastyczności (Effect of methodology on determining the Atterberg limits for liquidity index). *Civil Environ Eng* 4: 113–118.
21. Kostrzewski W (1988) Parametry geotechniczne gruntów budowlanych oraz metody ich oznaczania (Geotechnical parameters of soil and methods of theirs derivation). Poznań, Poland: Wydawnictwo Politechniki Poznańskiej.
22. Młynarek Z, Tschuschke W, Wierzbicki J (1997) Klasyfikacja gruntów podłoża budowlanego metodą statycznego sondowania (Soil classification by means of cone penetration testing), Gdańsk, Poland, 119–127.
23. Liszkowski J, Tschuschke M, Młynarek Z, et al. (2004) Statistical evaluation of the dependence of the liquidity index and undrained shear strength of CPTU parameters in cohesive soils. In: Viana da Fonseca A, Mayne PH, editors, 2014, Porto. Millpress, 979–985.
24. PKN (1981) PN-81/B-03020; Grunty budowlane. Posadowienie bezpośrednie budowli. Obliczenia statyczne i projektowanie (Polish standard PN/B-03020: Building soils. Foundation bases. Static calculation and design).
25. Lasowska A (2018) Analysis of spatial variability of Vistulian glaciation tills unt weight using CPTU probing. Poznań, Poland: Adam Mickiewicz University, 55.
26. Robertson PK (2009) Interpretation of cone penetration tests—a unified approach. *Can Geotech J* 46: 1337–1355.

27. Mayne PW (2014) Interpretation of geotechnical parameters from seismic piezocone tests. In: Robertson PK, Cabal KI, editors, USA: Las Vegas, ISSMGE Technical Committee TC 102, 47–73.
28. Marchetti S (1980) In situ tests by flat dilatometer. *ASCE Jnl GED* 106: 299–321.
29. Lunne T, Powel JJM, Hauge EA, et al. (1990) Correlation of Dilatometer Readings to Lateral Stress. Proc of Special Session on Measurement of Lateral Stress, Washington D.C.
30. Karlsrud K, Lunne T, Kort DA, et al. (2005) CPTU correlations for clays, Osaka. Millpress, 693–702.
31. Kulhawy FH, Mayne PW (1990) Manual on estimating soil properties for foundation design. Electric Power Research Institute, EPRI.
32. Młynarek Z, Wierzbicki J, Lunne T (2016) On the influence of overconsolidation effect on the compressibility assessment of subsoil by means of CPTU and DMT. *Ann Wars Univ Life Sci Land Reclam* 48: 189–200.
33. Młynarek Z, Wierzbicki J, Stefaniak K (2013) Deformation characteristics of overconsolidated subsoil from CPTU and SDMT tests. In: Coutinho RQ, Mayne PW, editors, Recife, Taylor & Francis Group, 1189–1193.
34. DeJong JT, Jaeger RA, Boulanger RW, et al. (2013) Variable penetration rate cone testing for characterization of intermediate soils. In: Coutinho RQ, Mayne PW, editors, Brazil: Recife, Taylor & Francis Group, 25–42.
35. Mayne PW, Peuchen J (2018) Evaluation of CPTU Nkt cone factor for undrained strength of clays. In: Hicks MA, Pisano F, Peuchen J, editors. *Cone Penetration Testing 2018*, London: Taylor and Francis Group, 423–429.
36. Stefaniak K (2015) Assessment of shear strength in silty soils. *Stud Geotech Mech* 37: 51–55.
37. Lechowicz Z, Szymański A (2002) Odkształenia i stateczność nasypów na gruntach organicznych (Deformations and stability of embankments on organic soil), Warszawa, Poland: Wydawnictwo SGGW, 184.